WOOD RESEARCH
59 (4): 2014
639-660

BEHAVIOUR OF TIMBER AND STEEL FIBRE REINFORCED CONCRETE COMPOSITE CONSTRUCTIONS WITH SCREWED CONNECTIONS

Eva Caldová, Lukáš Blesák, František Wald
Czech Technical University in Prague, Faculty of Civil Engineering
University Centre of Energy Efficient Building
Prague, Czech Republic

Michal Kloiber, Shota Urushadze
Academy of Sciences of Czech Republic, V. V. I., Institute of Theoretical and Applied Mechanics, Centre of Excellence Arcchip
Telč, Czech Republic

Petr Vymlátil
Designtec S.R.O.
Brno
Czech Republic

(Received February 2014)

ABSTRACT

This report describes the experimental work and numerical and analytical modelling of composite constructions consisting of a timber beam, a steel fibre reinforced concrete slab and shear connectors. The main aims of this work are the identification and the verification of parameters of contact elements that represent the connection, so that they could be used in complex numerical models of whole systems to explore the use of steel fibre reinforced concrete slab with timber beams and investigate the behaviour of the load floor structure using Ansys models. The results obtained in the numerical simulations are compared with the results obtained from push-out tests and the beam test. Six push-out tests and one beam test were conducted to determine the stiffness and the shear bearing capacity of the connection system under the application of steel fibre reinforced concrete. Based on the tests and FE modelling, the analytical model is prepared for the connectors of timber and steel fibre reinforced concrete composite beams.

KEYWORDS: Timber, steel fibre reinforced concrete (SFRC), screws, numerical model.

INTRODUCTION

Timber concrete composite constructions are used for various applications in the engineering industry, e.g. floor constructions or bridges. This technology is already quite well-known; the research has been made for over 30 years, especially for reconstructions of historical timber ceilings (Ceccotti 1995). At present, the research mainly focuses on the applications in multi-storey buildings and short bridges (Balogh et al. 2007).

Timber concrete composite slabs are made by connecting a layer of concrete with timber (beams). The concrete layer is mainly loaded in compression, while the timber beams are loaded in tension and bending (Ceccotti 2002). Shear strengths between these two components are transferred via the connecting system. The advantages in contrast to ceilings made of timber only are higher bearing capacity and greater stiffness, which lead to fewer deformations and a smaller inclination to vibrations with consequential better acoustic properties. The advantages also concern thermal properties and a better fire resistance (up to F30, F60 and F90), Fontana and Frangi (1999). The bottom part of concrete slabs is ineffective because they are cracked by tension and in the places of cracks moisture penetrates and the steel reinforcements corrode. By replacing the bottom parts of the slab with solid wood we can reduce the total thickness of the concrete slab by 50 %, reducing thus also the weight considerably (Gutkowski et al. 1999). If the solid wood is used for bridges, the corrosion of steel reinforcement is reduced as well as the degradation of the timber, the life of these elements is enhanced (Yttrup 1996). Greater stiffness minimizes deformations and enables a longer span of the designed constructions. In the case of traditional timber ceilings, the bearing capacity can be doubled and the stiffness is improved three or even four times (Stojit and Cvetkovie 2001).

Connectors of timber and steel fibre reinforced concrete composite beam the choice of connectors effective in shear is the key to strong and stiff compositeconstructions. efficiency of the shear connection can be measured based on Gutkowski et al. (1999):

$$\text{Efficiency} = \frac{D_N - D_I}{D_N - D_C} \tag{1}$$

where: DN - the theoretical full composite deformation (calculated starting at the transformed position),
DC - the theoretical full non-composite bending of a glued beam (the shear between layers is neglected),
DI - the real bending of the timber concrete composite beam.

In the case of a completely stiff connection without intermediate slip layers between the concrete and the timber, the efficiency can be between 0 and 100 %. To optimize the behaviour of a composite beam (slab), connectors with high efficiency should be used.

The most frequent methods of connecting concrete with timber were divided based on Ceccotti (1995) into 4 groups by connection stiffness. The smallest stiffness is manifested by steel connectors (nails, pole steel, bolts, etc.), which are of local character, are very malleable and flexible. Properties of connections depend on the distribution and geometry of these connectors, which provide the optimum work of the composite construction. Therefore, a high amount of such connectors are needed to achieve high efficiency (Deam 2007). Their advantage is that they are cheap and easy to install.

In 1990 the RF 2000 system (Meierhofer 1992) was introduced. This system was one of the first types of steel connectors made particularly for timber concrete composite constructions. The

connector, which has two heads, allows for the part between the heads to remain in the concrete layer and the rest is screwed into timber. Many researchers use this type of connector in their studies, including Steinberg et al. (2003), Frangi and Fontana (2003), Dias (2005).

A screw with high strength is nowadays used under the reference of SFS VB-48-7.5 x 150 mm. Steel connectors can also be of unlocal character, e.g., perforated metal, long bolts with split rings or steel tubes, etc. In contrast to the first group, these connectors have higher strength, ductility and tensile strength, as confirmed by Blass and Schlager (1997), Mungwa et al. (1999), etc. The reason is that nails and screws cause timber splitting, while tubular connectors provide more stiffness Clouston et al. (2004).

Another group of connectors involves tensile or prestressed bolts with shear grooves that are made in the contact surface of the timber element. Blass and Schlager (1997), proved that they have higher strength and resistance to slip than shear connectors made from tubes. The shear grooves can also be made by the mutual movement of several boards that are vertical and interconnected into a bearing element.

The last group of connectors based on Ceccotti (1995), has the highest stiffness. These are connections of metal elements secured by gluing. There is no slip between the concrete layer and the timber element. This connecting system manifests non-linear shear strengths even in the case of low values of loading (Piazza and Ballerini 2000; Steinberg et al. 2003). The usage of glue allows for the distribution of the shear strength evenly over the entire surface and thus reduces local concentrations of strength which appear when mechanical connectors are used. The connection by glue is non-slip and helps to reduce deformations. When gluing, the conditions during gluing and after gluing need to be considered (wood moisture content, conservation treatment, long-term behaviour of the system, etc.).

Satisfactory strength and stiffness are the most important properties for good timber concrete composite constructions. However, these properties are not a sufficient guarantee of success. When designing a timber concrete composite construction, it is necessary to consider other aspects besides strength and stiffness, such as ductibility and feasibility of the production and assembly. There is the rule – to achieve high strength and stiffness together with a simple and fast production and assembly, precast concrete slabs can be used (Crocetti et al. 2010). The greatest advantage of this way of connecting timber with concrete slabs is the dry assembly without technological delays (Collin et al. 2002). Recently, some studies have been conducted (Lukaszewska et al. 2006) at the Technical University Luleå, Sweden, focusing on the development of technologies for the connection of timber concrete composite constructions suitable for precast slabs only. The research has shown that there are great prospects of improvement but many tests still need to be performed to verify the achieved results.

Timber and steel fibre reinforced concrete composite constructions

The usage of steel fibres to reinforce timber concrete slabs seems promising as the construction units have a high tensile strength (Schafers and Seim 2011). Another advantage is that when the reinforcement by steel fibres is used, the concrete slabs can be very thin as the traditional steel rods are not necessary. The weight of the composite construction is thus considerably reduced (Kodur and Fike 2011).

The main effect on the efficiency of the timber concrete composite construction can be attributed to the connection between timber and concrete. Flexible connection by metal connectors, which is usually used, can lead to a reduced bending strength of the elements. Especially if the concrete slabs are reinforced by fibres, it is advisable, with respect to the high tensile strength of concrete, to use glue as the connecting agent so that a stiff composite

construction is achieved. At present, these applications are being researched.

Several research studies (Pham 2007; Lukaszewska 2009; Chataigner et al. 2011, Lie and Kodur et al. 1996) have focused on the classification of connectors: Local connectors (nails, bolts, screws, long bolts, etc.), which provide a limited construction stiffness; partially continual elements (a set of long bolts from expanded metal, etc.), whose stiffness properties depend on the distribution and geometry of elements; and construction gluing, which enables the optimum work of a composite construction (Fig. 1). It is important to realize that the construction gluing reduces the concentration of unfavourable phenomena compared to conventional methods. The stiffness of a glued connection depends on the stiffness of the glue used and the thickness of the glue layer.

The connecting system based on gluing manifests non-linear shear strengths and a relative slip relationship even for low values of loading (Piazza and Ballerini 2000; Steinberg et al. 2003). The usage of glue allows for the distribution of the shear strength evenly over the entire surface and thus reduces local concentrations of strength which is inevitable when mechanical connectors are used.

Analytical modelling of timber concrete composite beams

The design of timber concrete composite beams requires the knowledge of the behaviour of timber, concrete and shear connection. Depending on the complexity of the problem it is required to do certain simplifications to enable us to reach relatively easy solutions, the Eurocode 5-part 1-1, Annex b (Eurocode 5- 2003) provides a simplified calculation method for mechanically jointed beams. the simplified design method called "g method" is based on the approximate solution of the differential equation for beams with a partial composite action. According to the Eurocode 5 recommendations effective bending stiffness of a simply supported timber concrete composite beam with a cross section shown in Fig. 1 can be calculated as:

$$(EI)_{ef} = \sum_{i=1}^{3}\left(E_i I_i + \gamma_i E_i A_i a_i^2\right) \tag{2}$$

$$A_i = b_i h_i \,,\; I_i = b_i h_i^3/12 \,,\; \gamma_2 = 1 \tag{3}$$

$$\gamma_1 = \left[1 + \pi^2 E_i A_i s \Big/ \left(K_i l^2\right)\right]^{-1} \,,\; i = 1 \text{ and } i = 3 \tag{4}$$

$$a_2 = \frac{\gamma_1 E_1 A_1 \left(h_1 + h_2\right) - \gamma_3 E_3 A_3 \left(h_2 + h_3\right)}{2\sum_{i=1}^{3} \gamma_i E_i A_i} \tag{5}$$

where i - the number of elements (in the case of T–cross section i = 2),
E – modulus of elasticity of the concrete slab and timber beam,
γ_i – slip modulus of the mechanical fastener,
K_i – slip modulus of the connector,
l – beam length,
h_3 = 0 (for T–cross section).

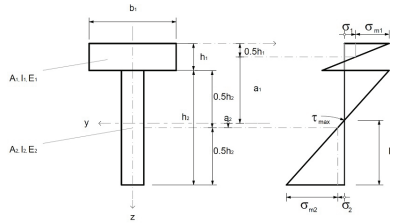

Fig. 1: Cross-section and bending stress distribution of a timber concrete beam.

The normal stresses can be calculated by these formulas:

$$\sigma_i = \frac{\gamma E_i a_i}{(EI)_{ef}} M \ , \ \sigma_{m,i} = \frac{0.5 E_i h_i}{(EI)_{ef}} M \tag{6}$$

The maximum shear stresses should be calculated as:

$$\tau_{2,\max} = \frac{\gamma_3 E_3 A_3 a_3 + 0.5 E_2 b_2 h_2^2}{b_2 (EI)_{ef}} V \tag{7}$$

The shear load on a fastener should be calculated as:

$$F = \frac{\gamma E_i A_i a_i s}{(EI)_{ef}} V \tag{8}$$

where: $i=1$ and 3, respectively;
sBiB=sBiB(x) - the distance between fasteners defined in B1.3.
and shear force in the cross-section is $V = V(x)$.

MATERIAL AND METHODS

The experimental program is divided into two main groups. The first group consists of tests of material properties and the second group contains tests of structural elements. Tests of material properties were standard cube compressive tests, standard cube tensile tests and four point bending tests at ambient and elevated temperatures. The aim of these tests was to assess the material properties of steel fibre reinforced concrete (hereinafter SFRC) for the analysis of mechanical behaviour of a timber concrete composite floor structure. Testing of structural elements consists of the push-out tests of connectors and the composite beam tests at ambient and elevated temperatures.

Material tests

The experimental programme started with material tests of SFRC at ambient temperature. Six standard cube compressive tests of compressive strength were performed in compliance with EN 12390-3 2009, as well as three standard cube tensile tests of tensile strength and three four point bending tests of tensile strength and ductility. Nine cubes with dimensions of 150x150x150 mm and three prisms with dimensions of 150x150x700 mm were made of each mixture. A series of fibre concrete specimens with a content of 70 kg·m^{-3} steel fibre strength of 1200 MPa and 1.5 kg·m^{-3} polypropylene fibres were tested. The average compressive strength at ambient temperature of 50.6 MPa was measured as well as the average tensile strength of 7.1 MPa under lateral tension.

The prisms were tested by the four-point bending test. The SFRC average tensile strength was reached at 4.34 MPa at a relative deflection of 1/824. The strain in the SFRC was calculated till the cracking limit state (CLS) occurred, Bednář (2013). At the level of initiation of macro-cracks the average ductility reached 1.71 ‰. After that, stretching increased and load bearing capacity decreased.

The concrete for all experiments was prepared in the concrete plant in Jindřichův Hradec, a small South Bohemian town, Czech Republic. The composition of the SFRC, which was used for the tests of the slab at elevated temperatures is summarised in Tab. 1.

Tab. 1: Composition of the tested SFRC.

Concrete plant ($kg.m^{-3}$)	Mixture 2012		Mixture 2013	
	JH	P	JH	P
CEM I 42.5 R Mokrá	330	330	330	330
Aggregate 0/4 mm Suchdol	948	-	948	-
Aggregate 0/4 mm Dobříň	-	948	-	948
Aggregate 8/16 mm Nemojov	669	-	669	-
Aggregate 8/16 mm Dobkovičky	-	669	-	669
Addition of fly ash Mělník	140	140	140	140
Addition ViscoCrete	3.96	3.96	3.96	3.96
Stachement MM	0.2	0.2	0.2	0.2
Water	190	190	190	190
Steel fibres HE 75/50 Arcelor	70	70	70	70
Polypropylene fibres	1.5	1.5	1.5	1.5

RESULTS AND DISCUSSION

Push-out tests of connectors

The mechanical behaviour of shear connectors between timber and fibre concrete has a igh influence on the performance of this type of composite structures. The parameters required to define the nonlinear behaviour of the connections are often not available, therefore the model input data are based on connector properties obtained from the experimental tests performed in compliance with ISO EN 26891 1991.

In order to determine the stiffness and shear bearing capacity of the connection system under application of fibre concrete, six push-out specimens were tested, see Fig. 2. The specimens were made of glue laminated timber GL24 h and concrete class C45/55 with steel fibres HE 75/50 Arcelor in a content of 70 $kg \cdot m^{-3}$ and with strength of 1200 MPa and 1.5 kg of polypropylene fibres 1.5 $kg \cdot m^{-3}$. As connectors TCC (Timber-Concrete-Connectors) screws Eurotec with diameter 7.3 mm and length of 150 mm were used in two rows; screws inclined 45 degrees with spacing of 100 mm in the longitudinal direction and 40 mm in the transverse direction. The slope of the screws in both lines was consistent and respected manufacturer's instructions.

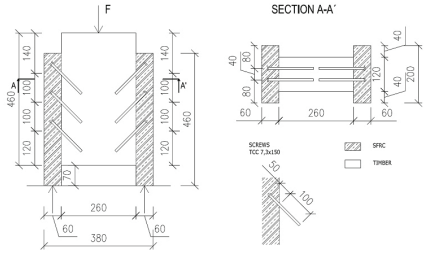

Fig. 2: The push-out specimen.

Fig. 3: The testing machine with a push-out specimen.

The load was increased force-controlled with a loading rate of 10 % of the estimated maximum load per minute. Within this loading regime the force was kept constant for 30 sec at

40 and 10 % of the estimated maximum load F_{est}. After that, further loading was applied path-controlled until failure or a displacement of 15 mm. This procedure assumes knowledge of the value of the estimated maximum load F_{est}.

The specimens were loaded in a servo-hydraulic testing machine and the loading regime was in compliance with ISO EN 26891 1991. Three specimens were tested in the first series of ST-1 and the second series ST-2. The first specimen of the ST-1 series was subjected to progressive loading with an estimated force F_{est} = 100 kN. The resulting force reached 255 kN, therefore the estimated force in further test was increased to F_{est} = 260 kN. To measure the displacement between the timber beam and the SFRC slab, four linear variable differential transformers (LVDTs) were applied, see Fig. 3.

The values measured from the four LVDTs of each specimen were averaged. Average values of vertical displacement and maximal force of both series are presented, see Fig. 4 and 5. The failure force is about 260 and 300 kN, respectively.

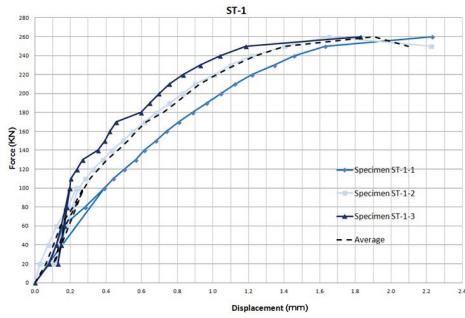

Fig. 4: Results of push-out test Series ST-1.

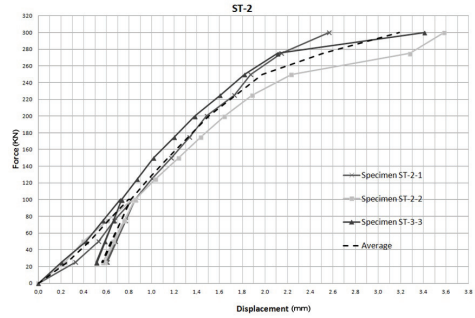

Fig. 5: Results of push-out test Series ST-2.

Composite beam test at ambient temperature

Test at ambient temperature

Bending test at ambient temperature was carried out to a simply supported 4.7 m span beam under static loading exerted on a typical four-point bending test configuration in an inverse position, see Fig. 6. The T-beam cross-section was made from glue laminated timber beam with the timber class GL36c, connected to a SFRC slab with fibre content of 70 kg·m^{-3}. The mid-span deflection and slip at the beam ends were recorded.

Fig. 6: The Four-point bending test configuration of a composite timber concrete T-beam.

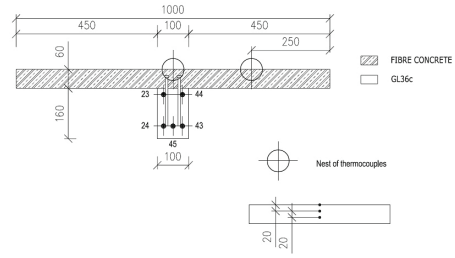

Fig. 7: The four-point bending test configuration of a composite timber concrete T-beam.

The beam was loaded with an increasing load until failure. The beam had a maximum deflection in the mid-span of 55 mm at the maximum force of the hydraulic cylinders 2 x 44 kN. In this deflection, a shear crack occurred in the timber beam, with a sudden drop in load force. After that the test was discontinued. The SFRC slab maintained its integrity during the test.

Test at an elevated temperature

The knowledge of fire behaviour of the timber concrete composite beam and the used mechanical connection was necessary to compare numerical predictions with experimental values. Based on the test performed at ambient temperature the same test was carried out at an elevated temperature. The specimens were composed of a glued laminated timber beam 100 mm wide and 160 mm high. A 60 mm thick SFRC slab was connected to a timber beam by 7.3 x 150 mm TCC screws with an inclination of 45 degrees to the beam axis in two rows. The temperature inside the timber beam was measured at the point of thermocouples 23, 24, 43, 44, 45, see Fig. 7.

The T-beam was loaded by nominal curve for 45 minutes. The beam was loaded continuously until failure force of 34 kN. This force was applied to the beam for 20 minutes before the start of the fire test to ensure the stabilization of the load and deflection.

Fire unprotected timber beam reached the highest temperature of 250°C in the mid-span of the beam in 20 min of the fire test. The maximum temperature in the concrete slab was 238°C and it was measured 20 mm from the bottom surface. The temperature rise at the unexposed face of the upper concrete slab after 20 min was slightly over 80° C.

The beam had a maximum deflection in the mid-span of 12.2 mm at the maximum power of the hydraulic cylinders 2 x 17 kN in 10 min of fire test. In this deflection a shear crack occurred in the timber beam, with a sudden drop in the load force. After that the structure was unloaded. Temperature measurement in the floor slab continued till the beam burnt. The SFRC slab maintained its integrity during the test.

Numerical modelling

The main purpose of this work is to analyze the behaviour of a timber SFRC composite beam with focus on the coupling elements. For this reason, both analytical and numerical models were made which are consequently compared to the laboratory tests of the subjected coupled beam. In order to understand the real behaviour of the self coupling and to be able to implement it into further calculations, various input data were compared one to another and results were concluded. For the numerical and analytical analysis, the same input data such as boundary conditions, type and value of loading, loading stages considering the initial and actual deformations, etc. were used, trying to simulate the real material and structural elements behaviour.

The results gained from a numerical and analytical calculation always need to be considered carefully, mainly in the case of a material such as timber and fibre reinforced concrete. Various factors mostly affected by timber defects and fibre concrete non-linear behaviour may bring more or less uncertain results, and this uncertainty has to be predicted and evaluated in the right way.

Model of push-out specimens

Input data

Material model for timber

Timber is a very complex material which is usually modelled on macro scale level as orthotropic, very seldom as an anisotropic linear elastic material model. In simulations where the failure of timber is expected either yield criteria for anisotropic plasticity, for example Hill yield criterion (Servít 1984) or even more advanced models with failure, according to Servít are used.

In fire simulations charring of timber parts which are exposed to fire takes place.

For the simulation of the composite floor slab, transversally isotropic material law with isotropic plasticity was used for timber parts. Data were adopted from EN 1995-1-1 2004 for glue laminated timber GL 24 h (modulus of elasticity parallel to grain 11 600 MPa, modulus of elasticity perpendicular to grain 390 MPa, shear moduli 720 MPa and tensile strength parallel to grain 16.5 MPa). The timber charring was taken into consideration as a reduction of elastic moduli and tensile strength due to temperature change. Curves for this behaviour were taken from EN 1995-1-2 2004, see Fig. 8. It is difficult to properly describe the dependency of anisotropic yield criteria on temperature, therefore only an isotropic yield criterion limiting tensile strength parallel to grain was used. The coefficient of thermal expansion of timber is lower thanfor SFCR so it does not play such an important role. Temperature dependency is not relevant either due to the fast thermal degradation and charring of timber, therefore only the constant value of 4.5E-6°C^{-1} was used for the coefficient of thermal expansion.

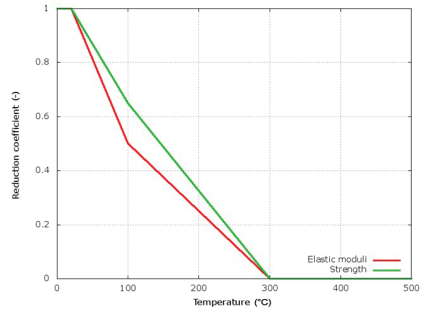

Fig. 8: Temperature dependent reduction coefficients for elastic moduli and strength of timber.

Material model for SFRC

To simulate the behaviour of the structure composed of SFRC and predict its fire resistance it is crucial to describe the main phenomena occurring in fibre concrete during the fire test by an appropriate material model.

Fibre reinforced concrete can be modelled at two different levels of observation, which are broadly categorized as micro-scale level and macro-scale level. Micro-scale models (more correctly denoted as meso-scale models) describe the phases of the composite material separately, i.e. fibre, aggregates, cement paste, and define interaction between them on the scale of the individual phases. Macro-scale models assume that the fibres and the matrix at this scale of observation are indistinguishable. In this context SFRC is considered as a homogeneous material. The advantage of meso-scale models is independent description of material properties of SFRC phases in contrast to the macro-scale models, where the material properties of SFRC depend on properties of the phases but also on the composition of the mixture. Therefore, it is often needed to obtain mechanical properties for macro-scale models for the calibration to a laboratory.

Modelling on macro-scale level was chosen for the description of a SFRC slab in the analysed structure as it is still more efficient for real structures. Laboratory tests were performed at ambient and elevated temperatures for the calibration of the material model, see chapter Material Tests.

Microplane model (ANSYS) was chosen as the most appropriate model available in ANSYS FE-code for modelling of SRFC exposed to fire. This model is suitable for modelling of damage due to extensive loading and thermal degradation. The material data for Microplane model were calibrated to measurements obtained from four-point bending tests at ambient and elevated

temperatures (see Fig. 9) and standard cube compressive tests.

Calibrated stress-strain curves for compression and stress-crack width curves for tension are shown in Fig. 10 for different temperatures.

Thermal expansion plays a very important role in the coupled thermo-mechanical analysis. Thermal expansion for siliceous concrete based on EN 1992-1-2 2004 was adopted for SFRC, see Fig. 11.

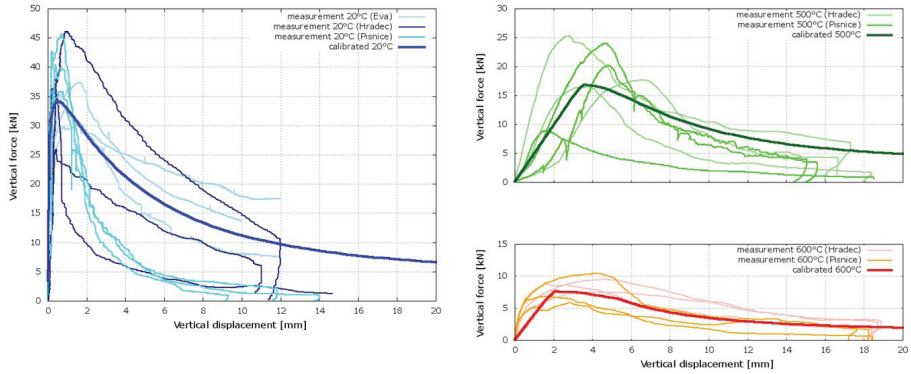

Fig. 9: Calibrated and measured force-deflection curves from the four-point bending test for ambient temperature (20°C) and elevated temperatures (500 and 600°C)

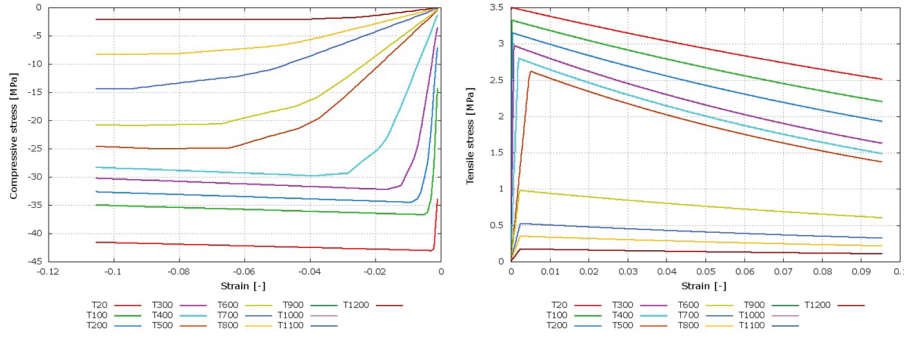

Fig. 10: Stress-strains diagrams for compression (left), stress-crack width diagrams for tension (right).

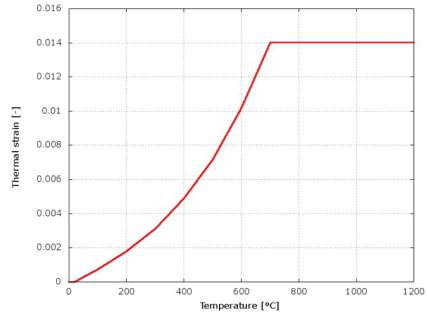

Fig. 11: Thermal expansion used for SFRC.

Load-displacement behaviour of timber fibre concrete composite specimens

In structural simulations of timber fibre concrete composite structures it is important to model the connection between timber and concrete properly. This connection in the analysed structure is made of screws as shown in Fig. 2. To obtain the shear stiffness and shear limit load of the connection push-tests were performed (see chapter Push-out tests of connectors). These tests were used for the calibration of connection in the numerical model of a floor slab. Shear stiffness and limit load of the connection is primarily determined by the strengths of connectors, anchoring depths and strengths of the base material. Friction effects between the connected parts take place only if their interfaces are under compression.

For the calibration of the shear behaviour two models of push-out test with different modelling of screw connection were carried out. The first model considered the screws to be beam elements embedded in concrete and timber, which are accompanied with nonlinear contact model with friction on the interface between timber and concrete (see Fig. 12). Such a model assumes only failure of screws due to plastic material law with hardening (see Fig. 13). This assumption corresponds to the results of push-out tests, where this failure mode was observed in all specimens. A much more detailed model would be necessary for more complicated failure modes, such as screw withdrawal. Still strength of the screws could be calibrated to shear load limited by withdrawal of screws from timber or concrete.

The second model assumes that screws are smeared to a special bonded contact model which can carry shear load with a defined strength, as shown in Fig. 12.

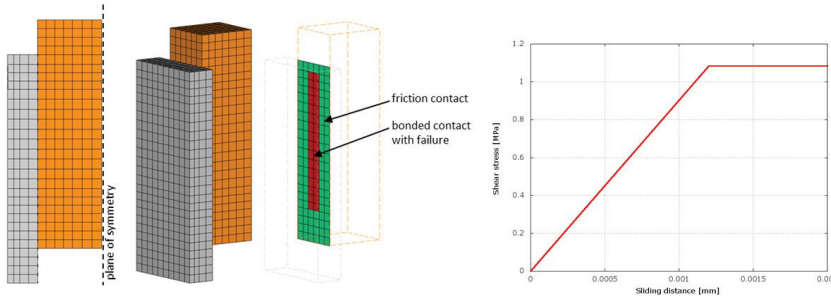

Fig. 12: The shear strength of this model has to be calibrated to the limit load due to failure of screws or withdrawal of the screws.

Both models were loaded by the prescribed displacement and the reaction force was measured. Material properties of both models were calibrated to the measured force-displacement curves. Results obtained from FE models compared with measurements are shown in Fig. 14. The performed numerical analyses proved the usability of both models in the mechanical simulation of the floor slab subjected to fire. The second model with smeared connectors was chosen for the analysis.

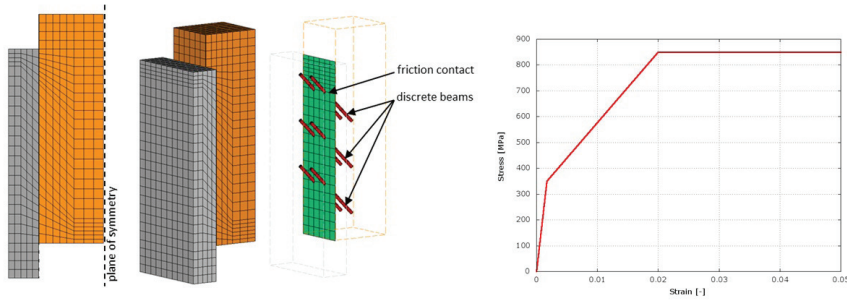

Fig. 13: Numerical model of push-out test with discrete connectors (left), stress-strain diagram used for discrete connectors (right).

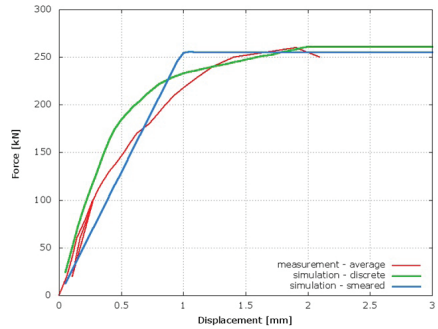

Fig. 14: Numerical model of timber concrete composite specimen and experimental load-slip curves for ST-1 test series.

Model of beams

Input data

Modulus of elasticity of timber

Modulus of elasticity of timber was measured by a four-point bending test, its self value being defined following the deflection of the middle part of the tested specimen (see Fig. 15). For the material tests we used specimens cut out directly from the tested beam after the self laboratory test in order to follow the real material behaviour as much as possible.

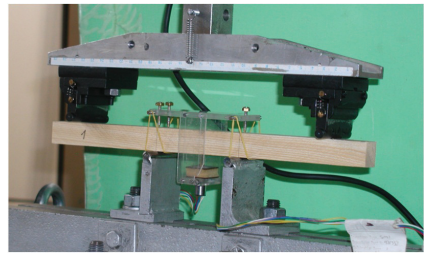

Fig. 15: Four-point bending test with respect to stress perpendicular to the grain flow failure.

One of the most influential effects over the calculated modulus of elasticity of timber in the

case of specimens with so small dimensions is the timber failure in compression perpendicular to the grain flow in the place of support. Compared to the middle span deflection, this value reaches approximately the same value and so the laboratory loading system was structured in the way to prevent the measuring device from measuring the support pressing into wood and to make sure only the deflection is measured.

Modulus of elasticity of timber was defined in its linear phase (behaviour of the tested beam was also linear during the loading test) as equal to 11.22 GPa. Timber density was defined to be 512 kg.m^{-3}.

Slip modulus of timber

Another major value resulted from the analytical and numerical calculation was the self value of slip modulus. Following the fact this paper mainly deals with an analysis of the effects of slip modulus or the connectors behaviour in SFRC, slip modulus values were gained based on three various elementary calculations.

- Slip modulus based on the standard calculation (Service ability limit state)

For this definition a standard calculation in compliance with the relevant code was used.

- Slip modulus based on a push-out test

Slip modulus and its definition by the laboratory push-out test and the consequent numerical simulation are listed in the previous chapters. Slip modulus of 17.54 kN·mm^{-1} was used in further calculations.

- Slip modulus based on the relative horizontal timber concrete movement

Horizontal slip movement in the coupling plane was constantly measured and used in the consequent analysis. Via defining a force applied on a connection element and the appertaining horizontal movement a slip modulus was defined for opted loading phases using the data gained from the laboratory experiment.

For this purpose, a measuring device was assembled at each end of the analyzed beam (as figured in Fig. 16) and the average value from both of the ends was used in further analyses.

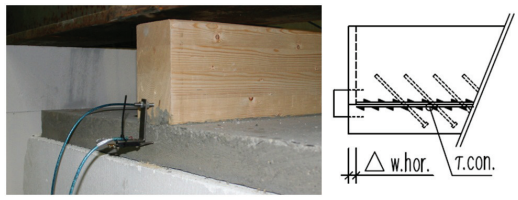

Fig. 16: Slip horizontal movement measuring.

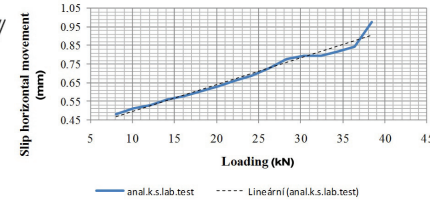

Fig. 17: Horizontal movement – loading diagram.

Slip horizontal movement evaluation

Slip horizontal movement Δw_{hor} was measured constantly during the self-loading experiment. When the loading intensity was equal to 0.4 x F_{max} (F_{max} = 44 kN), slip horizontal movement was Δw_{hor} = 0.755 mm. Using this value to calculate the correspondent slip modulus (ks), ks is equal to 7150 N·mm^{-1}. As this value can be defined after calculating the bending stiffness of the beam, it was needed to apply an iteration procedure. Partial values of slip modulus based on the horizontal movement in other opted loading stages are listed in Tab. 2:

Tab. 2: Horizontal movement correspondent to an appertaining loading.

Loading related to $F_{,max}$	0.1	0.2	0.3	**0.4**	0.5	0.6	0.7	0.8	0.9	1.0
k_s (kN.mm^{-1})	-	5.02	5.88	**7.15**	8.07	8.88	9.14	9.87	10.60	-
Δw_{hor} (mm)	0.29	0.60	0.70	**0.76**	0.82	0.87	0.95	0.99	1.04	1.25

In order to prevent evaluation of improper values, the extreme results appertaining to the loading 0.1 x F_{max} and 1.0 x F_{max} were not taken into account.

Fig. 17 shown the values of slip horizontal movement as a function of loading. As the vertical deflection increases it is clear that the slip horizontal movement increases as well, however, linear behaviour of vertical deflection progress is more obvious than slip horizontal movement progress.

Fig. 17 and Tab. 2 show that the mutual timber-concrete coupling expressed using a slip modulus value increases with an increase in the horizontal movement. Possible reasons for this action may be the wood hardening around the connector as it is pushed into the self material, yielding of the self coupling element, or the way SFRC behaves in such connections.

Modulus of elasticity of SFRC

A separate material test of SFRC to define its modulus of elasticity was not performed and so the modulus of elasticity for SFRC, based on the used concrete mixture, was considered to be $E_{fc,ck}$ = 36 GPa. As this experiment does not focus on the SFRC material behaviour, a linear stress-strain diagram was used for SFRC.

Model of beam

Before analysing a beam such as the one in this paper, it is necessary first to define the way of the self modelling and to decide if a 2D or a 3D model would be satisfactory for the expected results in order to verify them clearly and responsibly. As the results of the problem being solved will not vary as a function of the self beam thickness, a 2D model in Scia Engineer 2012 application was selected. Boundary conditions and other input data copy the ones in the laboratory test. A model such as this one enables deflections, both vertical and horizontal, to be verified and consequently compared to the ones gained by an analytical calculation using various input data. Slip modulus of the connection elements is represented by an interlayer placed between the concrete and the timber – in the place of the shear plane of the connectors, whilst its properties were modified to represent the real behaviour of the connectors. The properties were defined based on the push-out test mentioned in chapter Push-out tests of connectors. Material properties of timber and concrete were used the ones gained by a separate material tests. The same timber element as tested in the laboratory was consequently material tested.

When comparing the results, we opted to use only one representative loading stage. For this purpose, loading by two forces acting in the thirds of the theoretical span with a value of 36.4 kN was applied. The scheme of the numerical model with the appertaining boundary conditions and the applied loading can be seen in Figs. 18, 19.

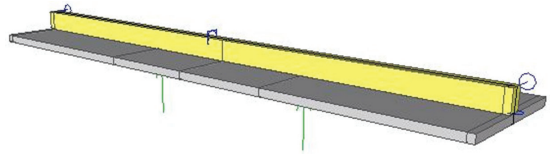

Fig. 18: Axonometric view of the numerical model.

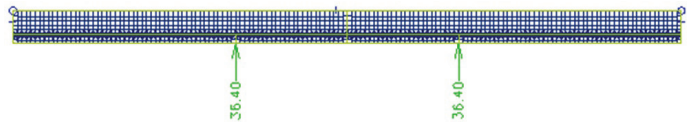

Fig. 19: Plane view of the numerical model (span = 4.5 m, nodal forces acting in the thirds of the span).

Considering the fact that the real beam was loaded by a steel profile with a contact area equal approx. to 100 mm x beam width and supported also approximately at the same contact area, the maximum stresses directly in these areas were not taken into account.

Evaluating the results

All the analysed results such as vertical deflection slip horizontal movement or shear stress in the coupling plane appeared to be very sensitive when varying the slip modulus input data changing the non-linear material properties of the interlayer in the coupling plane. Anyway, the interlayer was modified in the way so that the slip horizontal movement and the vertical movements are very close to the real slip horizontal movement. The possible inaccuracies may be caused directly by the non-linear behaviour of the coupling (Fig. 20).

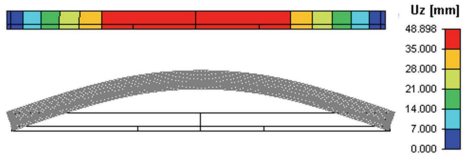

Fig. 20: Vertical deflection under the applied loading.

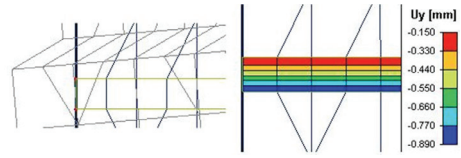

Fig. 21: Slip horizontal movement in the coupling plane under the applied loading.

Relative slip horizontal movement under the applied loading equals to 0.74 mm.

When such sensitive results as slip horizontal deflection are analyzed, it is necessary to consider the loading steps. Based on the loading phases, the initial slip horizontal movement and vertical deflection under the self weight loading were considered. These values were consequently implemented into the calculation of the particular values investigated in the particular loading steps. Values of the slip horizontal movement are shown in Fig. 21.

The results analysis mainly focused on the slip horizontal movement and vertical deflection. Vertical deflection needs to be evaluated considering the loading steps – mostly the initial deflection of the beam loaded by the self weight. Initial deflection was defined as being equal to 5.38 mm. As the self weight acts in the contra direction to the applied loading, the initial deflection was consequently subtracted from the evaluated values of vertical deflection.

Based on the loading steps, the force applied by the loading jacks has to be decreased by the beam dead-weight when loading the beam in the analytical calculation. The mentioned loading steps can be separated by defining two various loading cases in the software used.

Sensitivity study

As mentioned above, this paper focuses on an analysis of timber-concrete coupling, and so several input data were opted to be applied, such as modulus of elasticity of timber and SFRC, considering their approximate values to be linear. Even the slip modulus showed to be non-constant as the beam was loaded. Based on the standard calculation, even the numerical model

was made using a constant slip modulus. The sensitivity study serves to point out the effect of the usage of uncertain input data on the results compared to the laboratory experiment results. In the following table, the values analysed are presented and consequently compared to the real beam behaviour results.

An analytical model based on the correspondent codes was elaborated; however, the input data for the slip modulus varied. Consequently, the results can be compared in Tab. 3.

Tab. 3: The analyzed values from the applied calculation procedures and laboratory tests and their mutual comparison.

Analytical model with respect to k.s.EN								
Applied load related to F.max	20 %	30 %	40 %	50 %	60 %	70 %	80 %	90 %
Applied load 2 x F	8.1	12.13	16.18	20.22	24.26	28.31	32.35	36.4
k.s	7.36	7.36	7.36	7.36	7.36	7.36	7.36	7.36
w.max	11.27	16.87	22.5	28.12	33.74	39.37	44.99	50.63

Numerical model with respect to laboratory tests	
Applied load related to F.max	90 %
Applied load 2 x F	36.4
k.s	15.4
w.max = w (1.0 x load + self weight)	48.9
Δw.max = Δw.actual.	0.74

Laboratory test								
Applied load related to F.max	20 %	30 %	40 %	50 %	60 %	70 %	80 %	90 %
Applied load in one jack F.slf.i	11.66	15.69	19.74	23.78	27.82	31.87	35.91	39.96
App. load in a jack minus self weight	8.1	12.13	16.18	20.22	24.26	28.31	32.35	36.4
w.max = w.actual. - w.init. (5.38)	11.58	15.71	19.75	24.16	28.77	34.03	38.8	43.28
Δw.max = Δw.actual. - Δw.init. (0.2)	0.48	0.53	0.58	0.63	0.69	0.775	0.795	0.845

Analytical model with respect to k.s.lab.test - k.s defined based on Δw when force in a jack F.lsf.i = load + self weight (1/2)								
Applied load related to F.max	0.20	0.25	0.30	0.35	0.40	0.45	0.50	0.55
Applied load on a beam 2 x Fi	8.1	0.0	12.1	14.2	16.2	18.2	0.0	22.2
App. load in a jack F.slf.i	11.7	3.6	15.7	17.8	19.7	21.8	3.6	25.8
k.s	13.2	13.3	14.2	14.2	14.8	15.0	15.2	15.1
w.max	10.2	12.7	15.1	17.7	20.1	22.6	25.0	27.5
Δw.max = Δw.actual. - Δw.init. (0.2)	0.5	0.5	0.5	0.6	0.6	0.6	0.6	0.7

Analytical model with respect to k.s.lab.test - k.s defined based on Δw when force in a jack F.lsf.i = load + self weight (2/2)								
Applied load related to F.max	0.60	0.65	0.70	0.75	0.80	0.85	0.90	0.95
Applied load on a beam 2 x Fi	24.3	26.3	28.3	30.3	32.4	34.4	36.4	38.4
App. load in a jack F.slf.i	27.8	29.9	31.9	33.9	35.9	37.9	40.0	42.0
k.s	14.9	14.4	13.9	14.2	15.2	15.5	15.4	12.6
w.max	30.1	32.8	35.5	37.9	40.0	42.4	45.0	48.8

Δw.max = Δw.actual. - Δw.init. (0.2)	0.7	0.7	0.8	0.8	0.8	0.8	0.8	1.0

Units used in the Tab. 3: $k._s$ (kN.mm^{-1}), F (kN), deflections (mm)

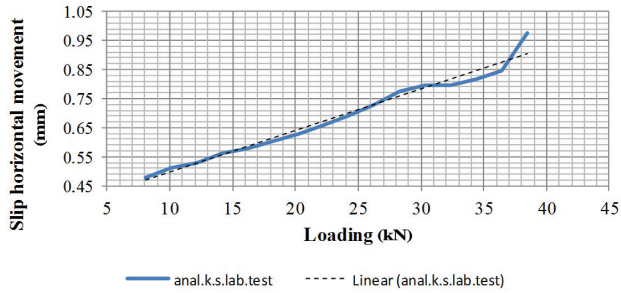

Fig. 22: Slip horizontal movement – loading diagram.

Even the vertical deflection appeared to be linear; the slip modulus changes during the loading experiment following a non-linear curve (see Figs. 22, 23).

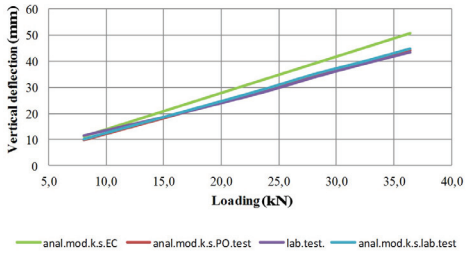

Fig. 23: Vertical deflection – loading diagram.

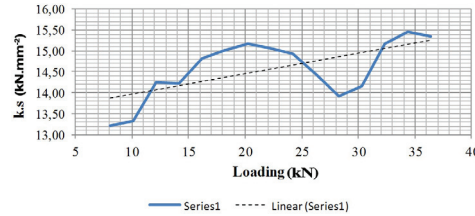

Fig. 24: Slip modulus – loading diagram based on the analytical model with respect to k.s.lab.test.

Besides slip modulus and the vertical and horizontal deflections, even the correspondent shear stress in the coupling plane was analyzed in the frame of the numerical model. Stresses in the particular directions in the coupling plane are shown in Fig. 25.

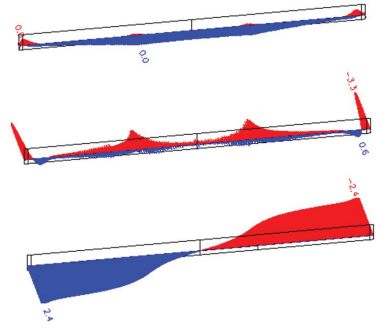

Fig. 25: Axial stress in the "x" direction (parallel to the beam axis) – up, axial stress in the "y" direction (transversal to the beam axis) – middle, stress in direction "xy" – down.

Analytical model

Based on the formula: $$\sigma_{xy} = \frac{1}{2}\cdot\left[\sigma_x + \sigma_y + \sqrt{\left(\sigma_x - \sigma_y\right)^2 + 4\cdot\tau_{xy}^2}\right] \quad (9)$$

and considering the zero values of axial stress in the "x" direction and low stresses in the "y" direction – not considering the stress tips in the places of the supports and the beam loaded, it can be stated that the "xy" stress figure represents the formula of shear stress on the coupling plane. When considering rectangular progress of "y" direction stresses, using formula (1) the average shear stress acting over one coupling element can be defined as follows:

$$\sigma_y := 0.4\text{MPa} \qquad \sigma_x := 0\text{MPa} \qquad \tau_{xy} := 2.19\text{MPa} \quad (10)$$

$$\sigma_{xy} := \frac{1}{2}\cdot\left[\sigma_x + \sigma_y + \sqrt{\left(\sigma_x - \sigma_y\right)^2 + 4\cdot\tau_{xy}^2}\right] = 2.4\text{MPa} \quad (11)$$

$$b_2 := 100\text{mm} \qquad s_{ef} = 50\text{mm} \quad (12)$$

Average force in one connector:

$$F_{av.con.} := \tau_{xy}\cdot b_2\cdot s_{ef} = 10.955\text{kN} \quad (13)$$

$$F_{d.max} := \frac{\gamma_{1POtest}\cdot E_1\cdot A_1\cdot a_{1POtest}\cdot s_{ef}}{EI_{eff.POtest}}\cdot F = 10.135\text{kN} \quad (14)$$

Based on the standard calculation, the maximum force in one connector is equal to 10.135 kN. The standard calculation considers a constant shear flow along the lateral thirds of the beam resulting in the constant value of shear force along the lateral thirds of the beam when loaded by two forces in the thirds of its span. This fact proves that the standard calculation can be considered to be reliable following the force value, however, not following the coupling elements loaded differently along the beam.

CONCLUSIONS

The positive effects of timber concrete composite constructions are well known around the world. Application of steel fibres as a replacement of conventional reinforcement to concrete mixture brings many advantages. However, the knowledge about this kind of structure is very limited although its potential is very high.

Therefore, the subject of this paper is load-displacement behaviour of composite timber and steel fibre reinforced concrete composite specimens. Material properties tests at ambient and elevated temperatures and push-out tests were made for the verification of the behaviour of timber and steel fibre reinforced concrete composite beam. Tensile strength and ductility of fibre reinforced concrete were measured. Based on the performed tests the numerical models of the timber and steel fibre reinforced concrete composite push-out tests and beams were prepared.

The numerical model of push-out tests and the beam described in this paper predict the experimental behaviour of timber and steel fibre reinforced concrete composite specimen very satisfactorily and its relative simplicity makes it a good method for designing timber and steel fibre reinforced concrete composite structures. Verification of the implemented material models by numerical simulation of the experiments was an integral part of the nonlinear analysis of the structural system.

The laboratory experiment was compared to the results gained from both numerical and analytical models, the opted values were analyzed, mainly focusing on the sensitivity effect of

the variation of the defined input data. When comparing such sensitive results, it is necessary to consider the loading steps very carefully.

It can be observed that the value of the slip modulus changes during the self loading, which can be also stated based on the slip horizontal movement. The values of slip modulus gained from the listed push-out test, analytical calculation and also based on the laboratory experiment are different, as expected. Following the vertical deflections, the maximum deflections can be observed in the case of the standard calculation.

The force acting on the connection element changes along the beam, whilst its self value is not exactly a function of a vertical force, as can be considered in an elementary calculation, but rather a function of the beam coupling stiffness.

Nevertheless, the observed data gained from the laboratory measurements were idealized as the analyzed movements, loading procedure and the beam supporting and loading system were not exactly symmetrical. Together with the material non-linear properties, the analyzed data can mislead the concluded ideas, therefore, as proved by this experiment, it is always necessary to predict the behaviour of a structure first, then assemble the laboratory set for a structure testing and define the most convenient calculation procedure in order to gain reliable results and conclusions.

ACKNOWLEDGMENTS

This research is carried out by the support of the research project of the Grant Agency of Czech Republic No. P105/10/2159 and by the European Union, OP RDI project No. CZ.1.05/2.1.00/03.0091 – University Centre for Energy Efficient Buildings and research supported by the project No. LO1219 under the Ministry of Education, Youth and Sports National sustainability programme I.

REFERENCES

1. ANSYS simulation software, Ansys Inc., Pennsylvania, U.S.A.
2. Balogh, J., Fragiacomo, M., Gutkowski, R.M., 2007: Influence of repeated and sustained loading on the performance of layered wood-concrete composite beams. Journal Structural Engineering 133(9): 1307–1315.
3. Bednář, J., Wald, F., Vodička, J., Kohoutková, A., 2013: Experiments on membrane action of composite floors with steel fibre reinforced concrete slab exposed to fire. Fire Safety Journal (59): 111-121.
4. Blass, H.J., Schlager, M., 1997: Connection for timber-concrete composite structures. In: International Conference on Composite Construction - Conventional and Innovative, Innsbruck, Austria.
5. Ceccotti, A., 2002: Composite concrete–timber structures. Progress Structural Engineering and Material (4): 264-75.
6. Ceccotti, A., 1995: Timber–concrete composite structures. In: Blass, H.J. et al. (eds.) Timber engineering, step 2, 1st edn. Centrum Hout, The Netherlands.
7. Clouston, P., Civjan, S., Bathon, L., 2004: Experimental behavior of a continuous metal connector for a wood-concrete composite system. Forest Products Journal 54(6): 76-84. ISSN 0015-7473.

8. Chataigner, S., Caron, J.F., Duong, V.A., Diaz, A., 2011: Experimental and numerical investigation of shear strain along an elasto-plastic bonded lap joint. Construction and Building Material 25(2): 432-41.
9. Collin, P., Stoltz, A., Möller, M., 2002: Innovative prefabricated composite bridges. IABSE Symposium, Melbourne, Australia.
10. Crocetti, R., Sartori, T., Flansbjer, M., 2010: Timber-concrete composite structures with prefabricated FRC slab" in 11th WCTE. Riva del Garda: International conference prooceding, 2010. Proceedings of: Proceedings of 11th WCTE, Riva del Garda.
11. Deam, B.L., Fragiacomo, M., Buchanan, A., 2007: Connections for composite concrete slab and LVL flooring systems. In: Material and Structural J. ISSN Pp 1871-6873.
12. Dias, A.M.P.G., 2005: Mechanical behaviour of timber-concrete joints. Ph.D. thesis, University of Coimbra, Coimbra, Portugal.
13. Eurocode 5 – 2003: Design of timber structures – part 1–1: General rules and rules for buildings, pr EN 1995-1-1.
14. EN 1995-1-1, 2004: Eurocode 5: Design of timber structures – Part 1-1: General – Common rules and rules for buildings.
15. EN 1995-1-2, 2004: Eurocode 5: Design of timber structures – Part 1-2: General – Structural fire design.
16. EN 1995-1-2, 2004: Eurocode 5: Design of timber structures – Part 1-2: General – Structural fire design.
17. EN 12390-3, 2009: Testing hardened concrete. Part 3: Compressive strength of test specimens.
18. Fontana, M., Frangi, A., 1999: Fire behaviour of timber–concrete composite slabs. In: Centre scientifique et technique du bâtiment (CSTB), Av. Jean Jaurès 84, Champs sur Marne, Marne La Vallée Cedex 2, France (eds.) Proc. of 6th international symposium on fire safety science (IAFSS), ENSMA, University of Poitiers, France. ISBN 0-925-223-25-5: 891–902.
19. Frangi, A., Fontana, M., 2003: Elasto-plastic model for timber-concrete composite beams with ductile connection. Structural Engineering International. Journal of the International Association for Bridge and Structural Engineering 13(1): 47-57.
20. Gutkowski, R.M., Thompson, W., Brown, K., Etournaud, P., Shigidi, A., Natterer, J., 1999: Laboratory testing of composite wood-concrete beam and deck specimens. In: Proc. RILEM symposium on timber engineering, Stockholm, Sweden, September 13-14. Pp 263-272.
21. Kodur, V.K.R., Fike, R., 2011: Enhancing the fire resistance of composite floor assemblies through the use of steel fibre reinforced concrete. Engineering Structures (33): 2870-2878.
22. Lie, T.T., Kodur, V.R., 1996: Thermal and mechanical properties of steel-fiber-reinforced concrete at elevated temperatures. Canadian Journal of Civil Engineering 23(4): 511-517.
23. Lukaszewska, E., Johnsson, H., Sthen, L., 2006: Connections for prefabricated timber-concrete composite systems. In: WCTE, 2006.
24. Lukaszewska, E., 2009: Development of prefabricated timber-concrete composite floors. PhD thesis, Department of Civil, Mining and Environmental Engineering Division of Structural Engineering, Luleå.
25. Meierhofer, U.A., 1992: A new efficient system for timber/concrete composite structural elements. Test, research and development. In: Proc of the 8th World Conference on Timber Engineering, Lahti, for the IUFRO S5.02, RF 2000. Pp. 383-393.

26. Mungwa, M.S., Jullien, J.F., Foudjet, A., Henteges, G., 1999: Experimental study of a composite wood-concrete beam with the INSA-Hilti new flexible shear connector. Construction and Building Materials 13(7): 371-382.
27. Pham, H.S., 2007: Optimization and fatigue behavior of wood-UHPC connection for new composite bridges. PhD thesis, National School of Bridges and Roads. (Optimisation et comportement en fatigue de la connexion bois-BFUP pour de nouveaux ponts mixtes). In: Ph.D thesis, Ecole Nationale des Ponts et Chaussées (in French).
28. Piazza, M., Ballerini, M., 2000: Experimental and numerical results on timber-concrete composite floors with different connection systems. In: '6th WCTE', proceedings of the world conference on timber engineering, Whistler Resort, British Columbia, Canada, CD.
29. Schafers, M., Seim, W., 2011: Investigation on bonding between timber and ultra-high performance concrete (UHPC). Constr Build Mater 2011(25): 3078-3088.
30. Servít, R., Drahoňovský, Z., Šejnoha, J., Kufner, V., 1984: Theory of elasticity and plasticity II. (Teorie pružnosti a plasticity II.) Praha: SNTL, 424 pp (in Czech).
31. Steinberg, E., Selle, R., Faust, T., 2003: Connectors for timber-lightweight concrete composite structures. Journal of Structural Engineering 129(11): 1538-1545.
32. Stojit, D., Cvetkovie, R., 2001: Analysis of a composite timber-concrete structures according to the limit states: Design and innovative methods in coupling of a timber and concrete. Facta Universitatis, Architecture and Civil Engineering 2(3): 169-184.
33. Yttrup, P., 1996: Concrete enhanced timber. In: Proceedings of into wood engineering conference, New Orleans, USA; 29-31 October, 5 pp.

Eva Caldová, Lukáš Blesák, František Wald
Czech Technical University in Prague
Faculty of Civil Engineering
University Centre of Energy Efficient Building
Prague
Czech Republic

Michal Kloiber, Shota Urushadze
Academy of Sciences of Czech Republic, V. V. I.
Institute of Theoretical and Applied Mechanics
Centre of Excellence Arcchip
Telč
Czech Republic
Corresponding author: kloiber@atlas. cz

Petr Vymlátil
Designtec S.R.O.
Brno
Czech Republic